## SECTION 3 71

GEOPHYSICAL INTERPRETATIONS — INTRUSIVE BODIES, BOUNDARIES AND STRUCTURES AT DEPTH . . . . . 71
DATA AND METHODOLOGY . . . . . 71
MAGNETIC INTERPRETATIONS . . . . . 72
Faulting . . . . . 75
Yarrol Fault (BR) . . . . . 75
Calliope North (CN) . . . . . 76
Calliope South (CS) . . . . . 76
Gracemere (GM) . . . . . 76
Rookwood (RW) . . . . . 76
Intrusives . . . . . 77
Bouldercombe Igneous Complex (BC) . . . . . 77
Rawbelle Batholith (RB) . . . . . 78
Diglum (Dl) and Kroombit Tops (KT) . . . . . 78
Diglum (DL) . . . . . 78
Eulogie Park (EP) . . . . . 80
Galloway Plains Igneous Complex (GP) . . . . . 82
Craiglands Quartz Monzodiorite (CIC) . . . . . 83
Glassford Igneous Complex (GF) . . . . . 84
Bajool (BJ) . . . . . 85
Basins . . . . . 87
Casuarina Basin (CB) . . . . . 87
Jim Crow Basin (JC) . . . . . 87
Nagoorin Basin (NB) . . . . . 87
Parkhurst ‘Basin’ (PB) . . . . . 87
Rossmoya Basin (RB) . . . . . 87
Stanwell Basin (SB) . . . . . 87
Yaamba Basin (YB) . . . . . 88
GRAVITY INTERPRETATIONS . . . . . 88
Faulting . . . . . 88
Intrusives . . . . . 88
Basins . . . . . 89
RADIOMETRIC INTERPRETATIONS . . . . . 89
AREAS PROSPECTIVE FOR MINERALISATION . . . . . 89

FIGURE

7. Locations for Geophysical Modelling . . . . . 73
8. Bouldercombe Igneous Complex (BC) . . . . . 78
9. Diglum (DL) and Kroombit Tops (KT) . . . . . 79
10. Eulogie Park (EP) . . . . . 81
11. Galloway Plains Igneous Complex (GP) . . . . . 82
12. Glassford Igneous Complex (GF) . . . . . 85
13. Bajool Quartz diorite — Cecilwood Quartz Diorite (BJ) . . . . . 86
14. Bouldercomb Igneous Complex prospective areas . . . . . 90
15. Diglum Granodiorite prospective areas . . . . . 91
16. Galloway Plains Igneous Complex prospective areas . . . . . 92
17. Glassford Igneous Complex prospective areas . . . . . 93
18. Bajool Quartz Diorite prospective areas . . . . . 94

TABLE

1. 2D Models . . . . . 74
2. 3D Models . . . . . 75
3. Fourier analysis of basins . . . . . 75

# SECTION 3

# GEOPHYSICAL INTERPRETATIONS — INTRUSIVE BODIES, BOUNDARIES AND STRUCTURES AT DEPTH

## Geophysical interpretation summarised from internal departmental report prepared by W. Stasinowsky, 1998; comments on relationship to geological mapping by C.G. Murray

Knowledge of the composition, structure and depth of burial of rock units is an important aspect of the analysis of mineral resources. Mineralisation is often associated with volcanic and plutonic rocks and/or structural conduits within rock units (eg faults, shear zones). Knowing where these rocks and structural features are located at exploration depths is significant for an assessment of undiscovered mineral resources.

In this section, results of an analysis of aeromagnetic and gravity data for the Yarrol assessment area has provided outlines of magnetic rock units, faults and basement. The analysis of geophysical data are used to produce a number of maps that:

1. reflect variations in density within the basement rocks and provide an interpretation of the potential 3D distribution of possible host rocks,
2. locate concealed plutons and pluton contacts, faults, shear zones and other major structural features, and
3. identify intrusive phases within igneous complexes and where possible suggest relative timing relationships.

Modelling of geophysical data has also been undertaken to suggest the depth of Tertiary basins and the nature and orientation of faults and subsurface intrusive contacts. Discussion is provided in the text of how analyses have been made and the results.

It needs to be recognised that the results in this section are solely derived from an analysis of geophysical data and that whilst elements of the study are supported by GSQ mapping, not all the interpretations are consistent with field observations and laboratory investigations. Comments on the relationship of the geophysical interpretations to geological mapping are in italics.

## DATA AND METHODOLOGY

The primary datasets for this study are the Departmental airborne geophysical survey undertaken in 1995 over the Rockhampton–Monto region and interpretations conducted as part of AMIRA Project 385 (Horton & others, 1993), which identified continental scale linears using 1:2 500 000 scale magnetic images. Magnetic and radiometric data collected as part of the Rockhampton–Monto survey in 1995 had a flight line direction of 045/225 degrees, flight line spacing of 400m, sensor height of 80m, magnetometer sample interval of 6–8m and spectrometer sample interval of 60–80m. The AMIRA images were produced from line data from the Bureau of Mineral Resources (BMR, now Geoscience Australia) and data digitised off BMR and open file Petroleum Exploration Society of Australia (PESA) contour maps, effectively compiling a large number of aeromagnetic surveys flown at different heights, different line spacings, with different

instruments and introducing complexity to the interpretation process. Gravity data were sourced from the GSQ digital regional dataset for Rockhampton–Monto–Mundubbera, which was produced in 1996 and used station intervals of 1–2km along roads in a 4x4km grid and includes 11km grid Geoscience Australia data and company data. Gravity data are distributed unevenly over Yarrol and, as a result, the reliability of the interpreted thickness and to some extent the basement gravity, varies from place to place. Ideally for a map at the scale of 1:100 000, data points are needed every 2km. For specific areas of interest the user should refer to the gravity station plot to determine local coverage (refer geophysics GIS). These data were used to produce a Bouguer gravity anomaly map and various derivative gravity maps. Computations were performed with a grid of 2km spacing. Thus, even in areas where the gravity data are spaced closer than 2km, features with characteristic dimensions less than ~6km are not accurately portrayed. For example, steep basin edges, such as those formed by steep angled faults will appear more gentle. To provide coverage in the north of the study area the Departmental datasets were supplemented with geophysical data sourced from company surveys provided to the GSQ in the late 1980s–early 1990s by various mining companies. Specifications for company geophysical data are varied.

The original datasets comprised images and vector datasets. The images and algorithms were run in ER Mapper Version 6.0, with relative paths in the algorithms. The vector files (.erv) were converted to shapefiles using ArcInfo Version 7.0. Descriptions of the images used in the analysis and the algorithms applied are provided in the accompanying Yarrol Geophysics GIS.

## MAGNETIC INTERPRETATIONS

The magnetic dataset was interpreted with the objective of identifying:

1. concealed intrusives; depth of cover over intrusive bodies; the nature of intrusive contacts; the relative timing relationships of different phases within intrusive complexes,

2. dip and nature of significant structural features, and

3. depth to basement and structural controls in Tertiary basins.

A range of images including first vertical derivative and artificial shade were used to interpret near surface faulting from the magnetics. Deeper faulting was interpreted using the gravity dataset (refer section — Gravity Interpretations).

To aid the interpretation of some anomalies and structural features, modelling was undertaken using Forward and Naudy modelling techniques as well as Fourier analysis. Geophysical modelling involves the comparison of geophysical results with the real earth situation. Forward modelling is the technique of determining the geophysical response to a given earth model. Conventional Forward modelling was performed using Encom's Model Vision software. Initial models started with vertical prisms and were modelled in 2.5D (cross-section with limited strike). Subsequent models used prisms with polygonal cross sections. Modelling required profiles to be extracted from the total magnetic image (TMI) grid. This approach proved satisfactory because of the large size of the bodies being modelled, although some degradation of results may have occurred at shallow depths.

Thirty-two 2D models were completed for 21 sites with several models generated at specific sites to explore different scenarios. Two 3D models were generated where it was difficult to achieve a satisfactory result using 2D. While most of the models had susceptibilities consistent with those measured in the field, some were higher by a factor of 2. These instances were interpreted to be the effect of magnetic alteration with the gradual dissipation of magnetite away from the source. In these cases, where there were no sharp contacts, the results generated by modelling were deeper than actual because of the need to fit a measured curve.

An additional 14 models used a Naudy based automatic depth calculation method to determine depth to magnetic source. AutoMag, an ENCOM software program, was used for the

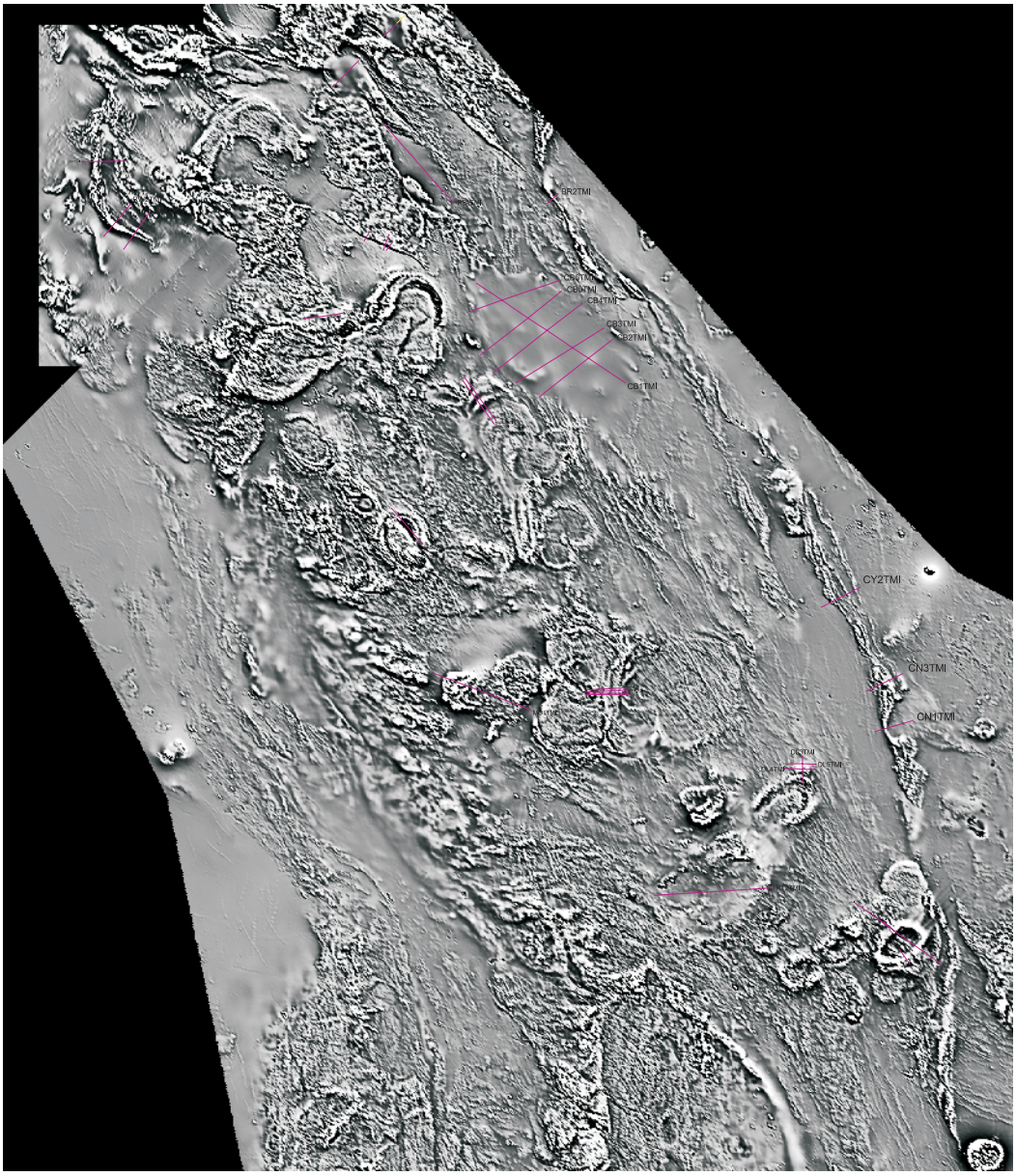


*Figure 7: Locations for Geophysical Modelling*

automated profile based (2D) depth estimation. This program compared the observed magnetic profile with theoretical anomalies to determine the depth and shape of the magnetic source. In AutoMag, one or more of the components of an anomaly edge can be adjusted to give a best fit. These components include: position, depth, dip and susceptibility. Because AutoMag was primarily used to determine the basement depth, the dip was usually fixed to vertical to minimise variables. AutoMag works on a finite number of samples within a spatial window. Samples were at 7.5m intervals and depths up to 2000m, with subsampling used to ensure sufficient width enough to cover anomalies from the desired depths. In some instances, this introduced variability in the depth estimates from noise in the profiles. AutoMag was run on several sections to give an assessment of depth to compare with results obtained from the Forward modelling and Fourier analysis. The models were saved as session files that contained both the data and the model as well as format information. These session files were prefixed with 'm' and had 'ses' extensions (refer geophysics GIS ). Raster bitmaps for some models have been hot linked in the geophysics GIS.

Modelling was conducted over the sites shown in Figure 7, see Tables 1–3.

Fourier analysis was conducted for flight lines over the selected basins to determine basement thickness.

Fourier analysis is based on the concept that a data series can be mathematically split into a

## Table 1: 2D Models

| Site | Model Name | Line Name | Start Coords | End Coords |
|---|---|---|---|---|
| Berserker Range | BR-A | BR2TMI | 263403E, 7417471N | 265408E, 7419158N |
| | BR-B | BR2TMI | " | " |
| | BR-C | BR2TMI | " | " |
| | BR-D | BR2TMI | " | " |
| Calliope-North | CY-A | CY2TMI | 311804E, 7346104N | 318858E, 7349693N |
| Calliope South Site 1 | CN-A | CN1TMI | 321328E, 7324072N | 328132E, 7326071N |
| Calliope South Site 2 | CN-B | CN3TMI | 319803E, 7331252N | 326353E, 7334377N |
| Casuarina Basin | CB-A | CB4TMI | 253908E, 7387471N | 269686E, 7399879N |
| | TMI*<br>TMI*<br>TMI*<br>CB-B*<br>TMI*<br>TMI* | CB1TMI<br>CB2TMI<br>CB3TMI<br>CB4TMI<br>CB5TMI<br>CB6TMI | 250868E, 7403413N<br>262044E, 7383280N<br>257853E, 7385745N<br>253908E, 7387471N<br>251690E, 7390676N<br>249635E, 7398318N | 277328E, 7385745N<br>275110E, 7393470N<br>273548E, 7395442N<br>269686E, 7399879N<br>266070E, 7402016N<br>265742E, 7403906N |
| Eulogie Park | EP-A | EP1TMI | 235956E, 7363663N | 241444E, 7357242N |
| | EP-B | EP1TMI | " | " |
| Galloway Plains | GP-A | GP3TMI | 270481E, 7330939N | 277906E, 7330939N |
| | GP-B* | GP3TMI | " | " |
| Craiglands | CIC-A | CIC1TMI | 243367E, 7334488N | 260581E, 7327884N |
| | CIC-A* | CIC1TMI | " | " |
| Glassford Site 1 | GF-A | GF1TMI | 325602E, 7285768N | 327585E, 7282876N |
| Glassford Site 2 | GF-B | GF2TMI | 322916E, 7290603N | 325870E, 7287979N |
| Glassford Site 3 | GF-C | GF3TMI | 317908E, 7293876N | 333113E, 7282933N |
| | GF-D* | GF3TMI | " | " |
| Gracemere | GM-A | GM1TMI | 234436E, 7409121N | 235630E, 7412107N |
| | GM-B | GM1TMI | " | " |
| | GM-C | GM1TMI | " | " |
| | GM-D | GM1TMI | " | " |
| | GM-E | GM1TMI | " | " |
| | GM-F | GM1TMI | " | " |
| | GM-G | GM1TMI | " | " |
| Kroombit Tops | KT-A | KT2TMI | 282355E, 7295136N | 303031E, 7296473N |
| | KT-B* | KT2TMI | " | " |
| Bajool | MG-A* | MG1TMI | 254111E, 7378468N | 248502E, 7386307N |
| | MG-B | MG1TMI | " | " |
| | MG-C | MG3TMI | 248817E, 7386814N | 254440E, 7378941N |
| Parkhurst 'Basin' | PB-A | PB1TMI | 234660E, 7431437N | 247049E, 7417406N |
| | PB-B* | PB1TMI | " | " |
| Rookwood Site 1 | RW1-A | RW1TMI | 181110E, 7424915N | 188809E, 7424996N |
| Rookwood Site 2 | RW2-A | RW2TMI | 185071E, 7411668N | 190007E, 7417582N |
| Rookwood Site 3 | RW3-A | RW3TMI | 188585E, 7409327N | 193212E, 7415877N |
| Rossmoya Basin | RB-A | RB9TMI | 234437E, 7446919N | 238453E, 7450838N |
| | RB-B* | RB9TMI | " | " |
| Stanwell Basin | SW-A | SW1TMI | 220504E, 7397065N | 227366E, 7398092N |
| Yaamba Basin | YB-A | YB9TMI | 225539E, 7437988N | 230261E, 7442839N |
| | YB-B* | YB9TMI | " | " |

* Modelling with AutoMag solutions superimposed

**Table 2: 3D models**

| Site | Model Name | Line Names | Start Coords | End Coords |
|---|---|---|---|---|
| Galloway Plains | GP-C | GP3TMI<br>GP5TMI<br>GP6TMI<br>GP7TMI | 270481E, 7330939N<br>270418E, 7330710N<br>270251E, 7331113N<br>270235E, 7331413N | 277906E, 7330939N<br>278003E, 7330710N<br>277594E, 7331446N<br>277494E, 7331930N |
| Diglum | DL-A | DL-3TMI<br>DL-4TMI<br>DL-5TMI | 308600E, 7319919N<br>305455E, 7317657N<br>306090E, 7318464N | 308651E, 7314675N<br>310869E, 7317400N<br>311061E, 7318341N |

**Table 3: Fourier analysis of basins**

| Site | Flight Line | Start Coords | End Coords |
|---|---|---|---|
| Casuarina Basin | 112140<br>112481<br>112580 | 251385E, 7395976N<br>260005E, 7385385N<br>275823E, 7395516N | 262035E, 7406684N<br>270357E, 7395746N<br>263003E, 7382671N |
| Jim Crow Basin | 111590 | 254000E, 7429711N | 260113E, 7435783N |
| Nagoorin Basin | 111590 | 328803E, 7300866N | 334028E, 7306110N |
| Parkhurst 'Basin' | 111430 | 237611E, 7422381N | 242758E, 7427455N |
| Rossmoya Basin | 110940 | 234501E, 7446962N | 239800E, 7452226N |
| Yaamba Basin | 110940 | 225594E, 7438077N | 230903E, 7443356N |

spectrum by applying the appropriate filter (a Fourier Transform). The resultant spectrum indicates the components of the original waveform in terms of the frequency and corresponding amplitude at each frequency. Applying this concept, the depth of a magnetic body can be determined from its measured profile. The broader the anomaly, the deeper the originating body. By assuming that a magnetic volcanic layer underlies sediments, the thickness of sediments can be determined by Fourier analysis of the magnetic profile to derive depth of sediment within a basin. The modelling process in this study used a sample interval of ~7.5m and had profile segments of ~7.7km and 15.4km. The magnetic profile data were imported into an Excel spreadsheet and the Fourier transform was computed.

Slopes were graphed using the formula:

$$\text{Depth} = \frac{(\text{Ln}(a) - \text{Ln}(b))}{4\pi(b - a)}$$

Where Ln(a) = Natural Log of Amplitude of First Point
Ln(b) = Natural Log of Amplitude of Second Point
a = Wavelength of First Point
b = Wavelength of Second Point

and by supplying intercept and slope values, which were manually adjusted to obtain a good fit for a spectrum segment. The more spectral points falling on the spectral segment and the more values agreeing in spectra on adjacent lines, the higher the confidence in the interpretation. The resultant model was an average for sediment thickness across a basin. Where the basin was faulted, the analysis was likely to show several depths. If the analysis could not resolve the different levels, the spectrum was considered to be inconclusive.

Modelling was also used to determine whether specific faults are normal, reverse or thrust. It needs to be recognised that modelling the lower boundary surface of magnetic bodies is difficult because variations in the overlying magnetic body may give rise to responses that are attributed to the lower surface. If the magnetic body is in the hanging wall, models attempting to fit faults to the lower surface are more ambiguous than models where the magnetic body occurs in the footwall or in basin depth determinations. Thrust interpretations made (refer geophysics GIS — Thrust.shp theme) provide a general indication of the thrust front and should be used in conjunction with the fault interpretation (refer geophysics GIS — faults.shp theme) because of the complexity introduced by high angle transverse faults.

## *Faulting*

### Yarrol Fault (BR)

Coordinate at approximate centre: 257 000 E, 7 425 000 N

Modelling was conducted to determine the dip of the main north-west striking fault. A number of models were constructed: fault with vertical dip, high-angle reverse fault dipping to the east, high-angle fault dipping to the west; and thrust (refer geophysics GIS — models BR-A to BR-D). The high-angle reverse fault dipping 75° to the east gave results most consistent with the data and agrees with current geological interpretations.

## Calliope North (CN)

Coordinate at approximate centre: 315 000 E, 7 349 000 N

Regional mappers interpreted this area as being thrust faulted. Forward modelling with shallow bodies dipping at 30° to the east fitted the data well.

## Calliope South (CS)

Coordinate at approximate centre: 323 000 E, 7 332 000 N

Modelling at Calliope South aimed at verifying an interpretation of thrust faulting in the area.

Line CS1TMI in the south intersected an interpreted thrust and an adjacent intrusion. Modelling of the data was consistent with bodies dipping to the east at 40° and suggested overthrusting of the intrusive. This interpretation is consistent with the weak response of the intrusion and its apparent lack of extent at depth.

*(An alternative interpretation is that the low magnetic response of the intrusion may be due to its low susceptibility.)*

Line CS3TMI traversed an interpreted multiple thrust package. Modelling highlighted deep vertical bodies to the west in the footwall block. A series of shallow bodies dipping at 30° to the east represented the thrust package and fitted both the leading and trailing parts of the data. Modelling the area to the east gave 60° dips to the east, suggesting that this area is either a steeper part of the thrust package or a different unit.

## Gracemere (GM)

Coordinate at approximate centre: 230 000 E, 7 412 000 N

Normal and thrust faulting has been suggested in the Gracemere area, consequently several scenarios were modelled with the following results:

1. simple bodies with an easterly dip of 40° fitted better than either vertical or westerly dipping bodies (refer geophysics GIS — models GM-A to GM-C)

2. vertical bodies truncated by a thrust achieved a good match with the exception of the prominent low (refer geophysics GIS model GM-D). Three other versions of the thrust model were produced (refer GIS models GM-E to GM-G) all having the western apexes shallower than the rest of the bodies. The evidence generated from these models suggests thrust faulting dipping to the east and steepening near outcrop.

*(Thrust models are inconsistent with geological evidence because the thrust package consists of late Cretaceous basalts. No significant post-Cretaceous thrusting is known in the terrane, only normal and strike-slip faults are recorded.)*

## Rookwood (RW)

Coordinate at approximate centre: 188 000 E, 7 413 000 N

Modelling was undertaken to determine if thrust faulting is present on the western edge of a shallow magnetic unit in the Rookwood area. In plan, the structure has the character of a thrust with a curved front and several cross-cutting faults, this has been interpreted as transverse faults in a thrust system. The transverse faults strike north-east.

Modelling on line RW1, in the north, gave good fits for tabular bodies with steep dips (refer geophysics GIS — model RW1-A). The western bodies have dips of 82° to the east while the eastern body has a dip of 75° to the west, suggesting a syncline. The interpretation of the western bodies however, is ambiguous as the low to the west did not fit well and the three adjoining bodies had varying susceptibilities. A more gentle dip to the east fitted the low better but failed to fit the high. The eastern body unambiguously dips west and is inconsistent with a thrust.

The second line, RW2 transects the highest magnetic response in the area, coinciding with a change in the trend of the fault. The profile

exhibited a broad low to the south-west which suggested normal faulting.

A third line further south was also modelled. RW3 provided a good fit to models with dips of ~45° to the south-west (refer GIS model RW3-A).

The Rookwood fault system had little evidence for thrusting, with modelling suggesting normal faults dipping to the west and south-west.

*(This region is in the Gogango Overfolded Zone for which structural interpretations indicate stacked thrust sheets dipping to the east.)*

## *Intrusives*

Intrusions in the Yarrol assessment area were interpreted using a TMI and first vertical derivative (refer geophysics GIS — theme dk_a.alg), greyscale first vertical derivative (refer geophysics GIS — theme dk_b.alg) and TMI on TMI vertical shade (refer geophysics GIS — theme dk_c.alg). Several intrusive complexes had detailed interpretations made as to the timing of their various phases and in some cases modelling to determine their extent at depth. The following text discusses the results of the detailed interpretations, also shown on the 'intrusions.shp' theme in the GIS.

### Bouldercombe Igneous Complex (BC)

There are two exposed or near surface lobes to this complex, which forms a dumbbell shape striking approximately east–west (refer geophysics GIS — theme bc_a.alg).

Coordinate at approximate centre of western lobe: 216 000 E, 7 390 000 N

Coordinate at approximate centre of eastern lobe: 239 000 E, 7 398 000 N

These major bodies are composed of a number of distinctive magnetic responses interpreted here as intrusive phases. Intrusive bodies associated with this complex are also interpreted to extend at depth to the north (refer geophysics GIS — themes bc_b.alg and bc_c.alg).

Timing relationships have been interpreted between the various phases as follows (refer geophysics GIS — theme bc_d.alg and Figure 8).

Body 1 does not crop out. It is the largest intrusive phase and extends north-south 18km and east-west 34km, dipping to the north-east and extending under a thrust front at Gracemere. It is interpreted as a composite body composed of four parts (1a–d), which most likely represent different depths of the same unit. It is unclear in the case of 1d whether the response represents a shallow part of body 1 or a different intrusion or possibly magnetic enhancement, the result of alteration. Body 1 is interpreted to be the oldest phase being intruded by bodies 2, 8 and 15. The northern and eastern boundaries are uncertain as they are very deep. At the western edge of the Bouldercombe Igneous Complex, body 3 is considered to be intruded by 4, which also intrudes 2. No clear relationship could be established between body 1 and 3. Bodies 3, 4 and part of 2 do not crop out.

Body 5 is interpreted to intrude 4 and 2 with body 5 intruded in turn by 6.

*(Body 5 corresponds to the foliated Flaggy Quartz Monzodiorite which is intruded by body 6, the Umbrella Granodiorite.)*

Body 7 intrudes both 6 and 5 and is interpreted to be a separate phase to 5 based on the differences in response identified on the southern margin of 7. *(Body 7 largely corresponds to the Moonkan Granite which is interpreted to intrude the Umbrella Granodiorite.)*

Body 8 is interpreted as being composed of 4 parts (8a–d) and to have been emplaced with a negative remanence. Part 8d has a particularly strong negative and may be a separate intrusion. *(Body 8d equates to the Quarry Gabbro. Body 8a equates to the Gracemere Gabbro.)* Bodies 10, 11 and 5 are similar in character. Body 10 intrudes 8 and possibly 9. *(Body 10 equates to the Bundaleer Tonalite, and body 9 to the Gavial Gabbro.)* Body 11 intrudes 2 but probably not 7. *(Body 11 is largely unexposed.)*

Body 12 is quite distinctive and is interpreted to intrude bodies 8, 9, 10 and 11. *(Body 12 is currently mapped as the western part of the Bundaleer Tonalite.)* Small intrusions 13 and 14 are interpreted to be later than 11 and 12. Body 13 occurs adjacent to 11 and possibly intrudes it, while 14 intruded 8 and 12. Body 15 is highly magnetic which is attributed to a magnetic aureole associated with the emplacement of bodies 8, 10 and 12. *(Body 15 broadly equates to the Kabra Quartz Monzodiorite.)* A magnetic high that intersects the magnetic

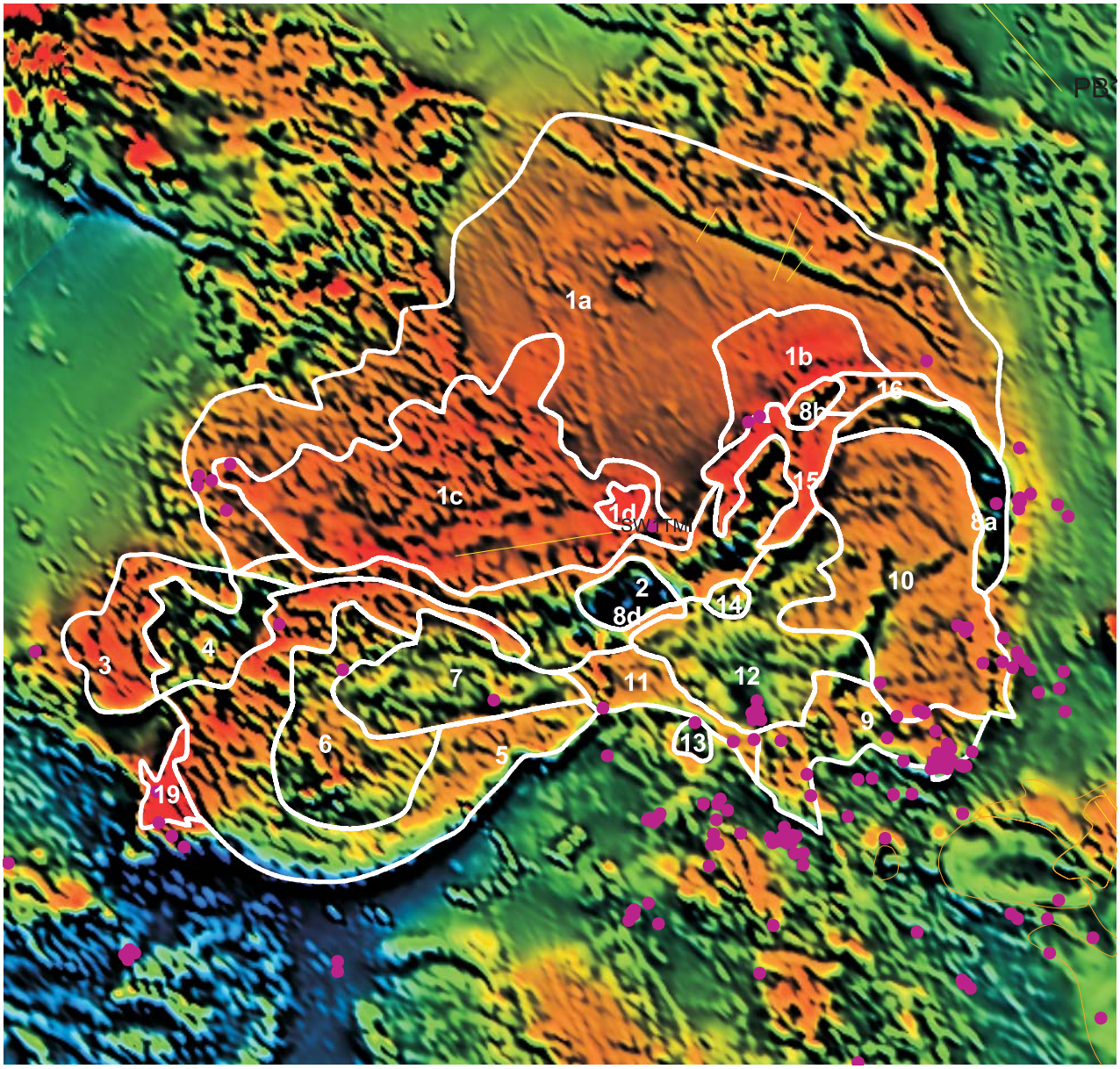


*Figure 8: Bouldercombe Igneous Complex (BC)*

lows of body 8 is considered to reflect alteration effects along a fault, either resetting the magnetic remanence and/or emplacing additional magnetite.

Body 16 may be a separate intrusive event, between 8a and 8b, or may be a response to alteration. *(Body 16 is mapped as part of the Gracemere Gabbro, which exhibits both positive and negative remanence. Body 19 is the strongly magnetic Bucknalla Gabbro, which is not regarded as part of the Bouldercombe.)*

## Rawbelle Batholith (RB)

Coordinate at approximate centre: 285 000 E, 7 255 000 N

The Rawbelle Batholith extends into the southern part of the Yarrol assessment area. It has a significant gravity low, an obvious magnetic rim and displays little internal magnetic variation.

## Diglum (Dl) and Kroombit Tops (KT)

Diglum (centred: 306000E, 7312000N), Diglum West (centred: 291000 E, 7311000 N) and Kroombit Tops (centred: 293000 E, 7296 000 N) form an interconnecting series of intrusions.

## Diglum (DL)

Body 1 (292700E, 7317000 N) and body 2 (308600 E, 7317800 N) correspond to shallowly buried areas in the complex. Detailed inspection revealed both these areas of magnetic highs are composite bodies and have their margins structurally controlled. Many of the faults postdate the intrusion, as evidenced

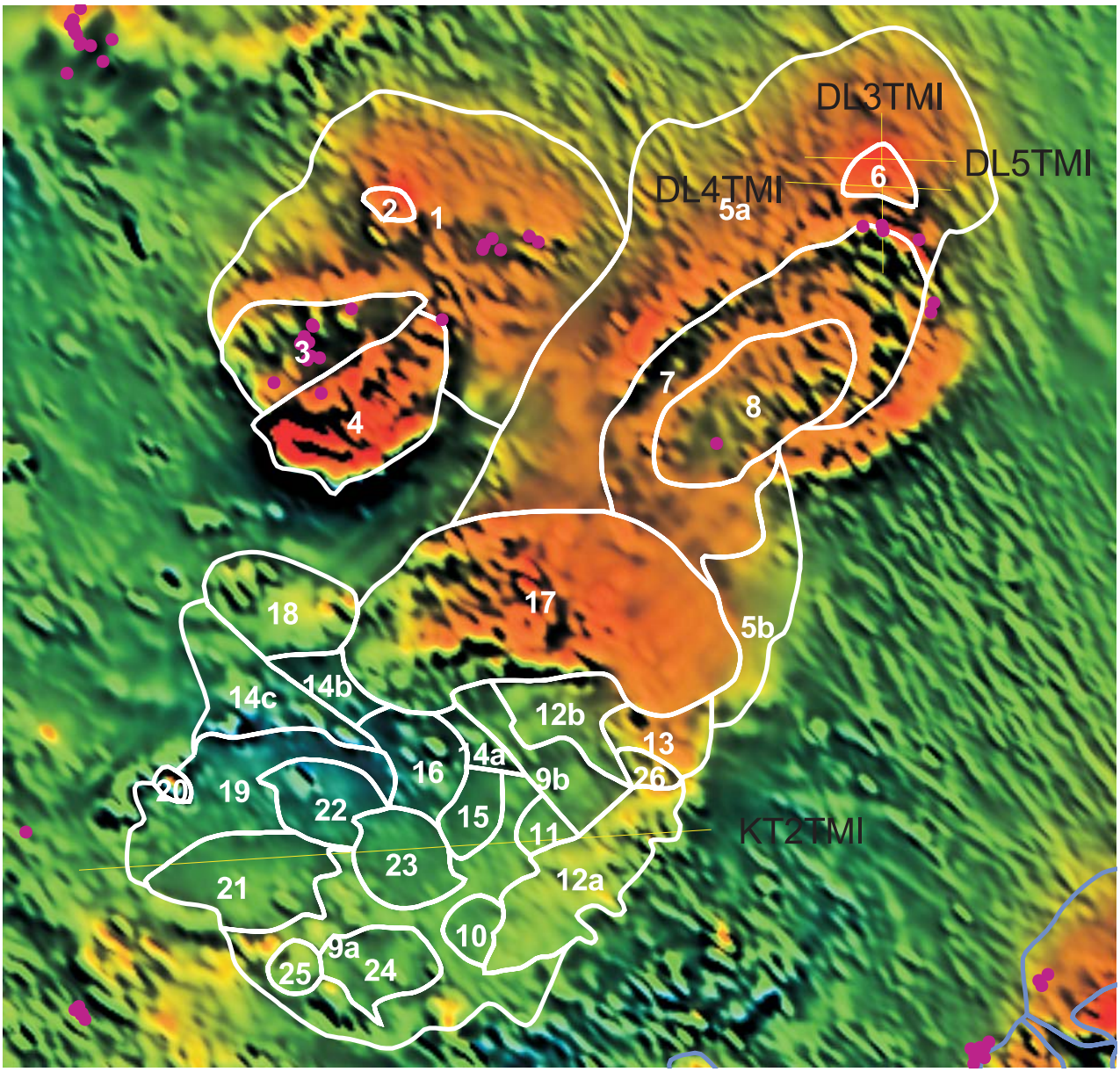


*Figure 9: Diglum (DL) and Kroombit Tops (KT)*

by margins displaced by faults. The intense magnetic highs are likely the result of one or a combination of three scenarios:

1. a very magnetic intrusion such as a gabbro or a near surface extension of a deeper intrusion,

2. skarns developed above a deep intrusion, which may be preferentially developed along structures,

3. structures hosting magnetic alteration emplaced by solutions derived from intrusions at depth and/or from dewatering of surrounding units.

Deeper intrusions are evident as broad areas of high magnetic signature. The margins of these deeper bodies are hard to map because of shallow dips, which make it difficult to detect sharp changes in magnetic level and because of the ambiguity of mapping the margin of a 3D body in 2D. Consequently, the interpreted margin reflects the maximum extent of the body.

Modelling was conducted in 3D on body 1 (refer geophysics GIS — model DL-A). Depths in the model range from 100–320m. The greater depths are probably an over estimation of the actual depth due to the variability of susceptibilities. Depths of between 100–200m are considered more likely.

The timing of the various intrusive bodies (refer geophysics GIS — theme dk_d.alg and Figure 9) is uncertain. Body 1 is considered to

be the earliest phase because it is intersected by all other bodies. Body 2 may be an extension of body 1 or could postdate it. *(The interpretation of body 1 is based purely on geophysics, with no surface expression. Body 2 has been mapped as an unnamed granodiorite.)* Bodies 3 and 4 are interpreted to be structural modifications of the same phase. If this is the case, the magnetic aureole associated with body 3 would originally have covered 4 as well. To derive the current response would require subsequent down faulting of the southern half of the emplaced intrusion, which would have preserved the covering aureole in the south but exposed it to erosion in the north. Bodies 3 and 4 intersect body 1. *(Bodies 3, 4 are mapped as granitic and dioritic phases of the Seaview Igneous Complex. The magnetic aureole to the north of body 3 is also diorite. The magnetics indicates a subsurface extension of the diorite to the south.)*

Intrusions 5a and 5b are interpreted to be the same body based on a similar depth and form. Body 6 postdates 5a unless it represents a shallow extension of the same. Both 6 and 5 intersect body 1. Body 7 has a significant aureole. Body 8 is contained within body 7 and is interpreted as a separate event because its southern boundary does not parallel that of body 7. *(Bodies 7 and 8 correspond to two phases of the Diglum Granodiorite and body 6 is probably a separate gabbroic intrusion to the north. These are surrounded by a strongly magnetic contact aureole in the Mount Mount Alma Formation and Rockhampton Group that represents the inner part of body 5.)*

Kroombit Tops consists of a series of intrusive phases that are interpreted to postdate the intrusions that occur further north in the Diglum area.

Individual anomalies were modelled to determine the depths to the top of the magnetic aureoles surrounding each phase (refer geophysics GIS — model KT-A). To gain information about the more subtle anomalies in the Kroombit area, AutoMag was run using sensitive settings (refer geophysics GIS — model KT-B). Results from all modelling indicated that the eastern side of the intrusives in the Kroombit Tops area are subcropping, with depths progressively increasing westwards to a maximum of ~200m in the centre of the magnetic feature.

Timing relationships between phases and the relationship to the Diglum intrusives are as follows (refer geophysics GIS — theme dk_b.alg and Figure 9). Intrusion 9, a composite body with parts a and b, appears to be the oldest phase in the Kroombit Tops complex. It is intersected by most other bodies in the area. Parts 9a and 9b are separated by a fault boundary but are interpreted to be the same phase based on their similar magnetic character. Body 14 is also a composite with three distinguishable parts (a–c) that are also all considered to represent a single phase based on their similar magnetic responses. Bodies 14 and 9 may be the same phase although there does appear to be some difference in their magnetic relief. Body 5b is intersected by body 13. Body 17 intersects both 5 and 7 suggesting that, at least in part, the Kroombit Tops intrusives are younger than the Diglum intrusives. No timing relationship could be established between bodies 13 to 17 and Diglum bodies 2, 3, 4, 6, 7 and 8. No relationship could be established between any of the Diglum phases and bodies 9, 10, 11, 12 and 14. Bodies 10 and 11 intrude 9a, all of which are intruded by body 12. Body 12 is composite with parts 12a and 12b identified and considered to represent the same phase because of similar magnetic responses. Body 13 a more magnetic body is considered a separate phase that intrudes 12b. Body 15 intrudes 9a and has a faulted boundary with 14a. Body 15 is intruded by 16, which also intrudes 14a and 14b. Body 17 is considered to be a shallow body intruding 12, 13, 14 and 16. It is in turn intruded by 18, which has faulted boundaries with 14. Body 19, an intrusion with some magnetic aureole development, is interpreted to intrude 14 and 16. Body 20, has an intense magnetic response, and may be similar to bodies 1 and 2. Body 20 intrudes 19. Body 21 is interpreted as intruding 20 and is in turn intruded by 22. Body 23 intrudes 22, 16 and 9a. Body 24 intrudes 9a and is intruded by 25. Body 26 shows a strong magnetic aureole. The western boundary is faulted, probably after emplacement as the aureole is absent here. Body 26 intrudes both 12a and 13. *(This interpretation is based purely on geophysics, with no surface indications of intrusions. The area is covered by Triassic volcanics.)*

## Eulogie Park (EP)

Coordinate at approximate centre: 237 000 E, 7 358 000 N

The Eulogie Park intrusive complex is dominated by a strong central negative magnetic response and a major fault that cuts the complex.

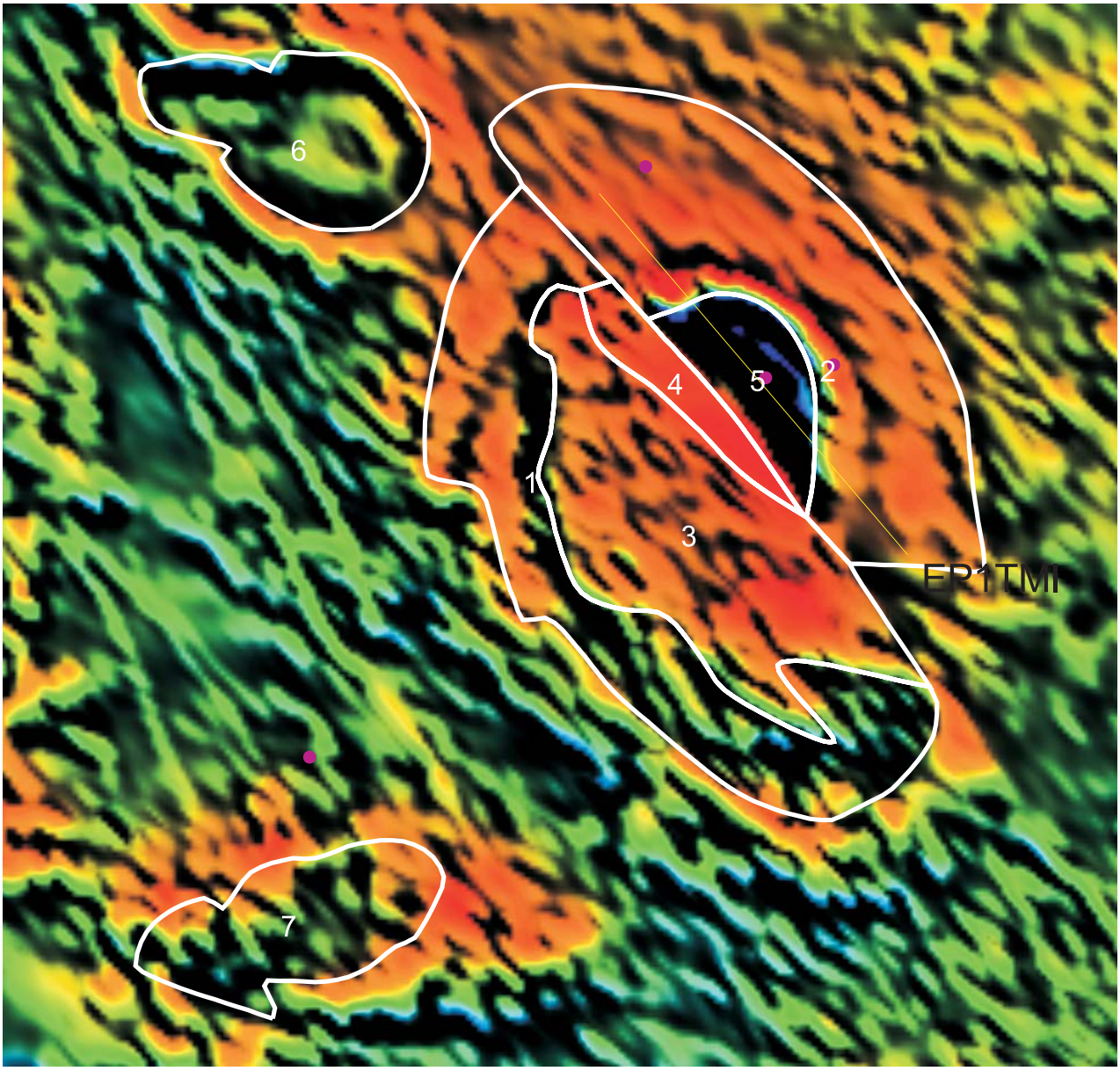


*Figure 10: Eulogie Park (EP)*

Relative timing relationships are as follows (refer geophysics GIS — theme ep_c.alg, ep_b.alg and Figure 10). Body 1 was emplaced first. A major fault separates body 1 from 2. The susceptibility of body 2 is similar to body 3 suggesting the same rock type. Alternatively, body 2 could be the same phase as body 1, but this scenario would require significant vertical displacement.

Body 4 has significantly stronger susceptibility and a different radiometric response to both 3 and 5. It is considered likely to be a part of a separate intrusion that has experienced vertical displacement emplacing the narrow sliver in its current location. Body 5, with a strong negative magnetic and distinctive radiometric responses, is also interpreted to be a separate intrusion. The western margin of 5 is faulted with significant vertical displacement. No relationship could be established between bodies 4 and 5.

Two 2D models were generated across body 5 to determine the nature of the margins and depth of cover. The first model used strikes perpendicular to the traverse. The second used strikes more consistent with the image interpretation. Results have the shallowest depth on the northern margin at 220m while negative anomalies in the south are more consistent with depths ranging from 320–450m. The deeper central anomalies generated depths ~500m.

*(Mapping indicates body 5 to be a layered gabbro with reverse remanent magnetism. The outer rim of this layered gabbro has positive remanent*

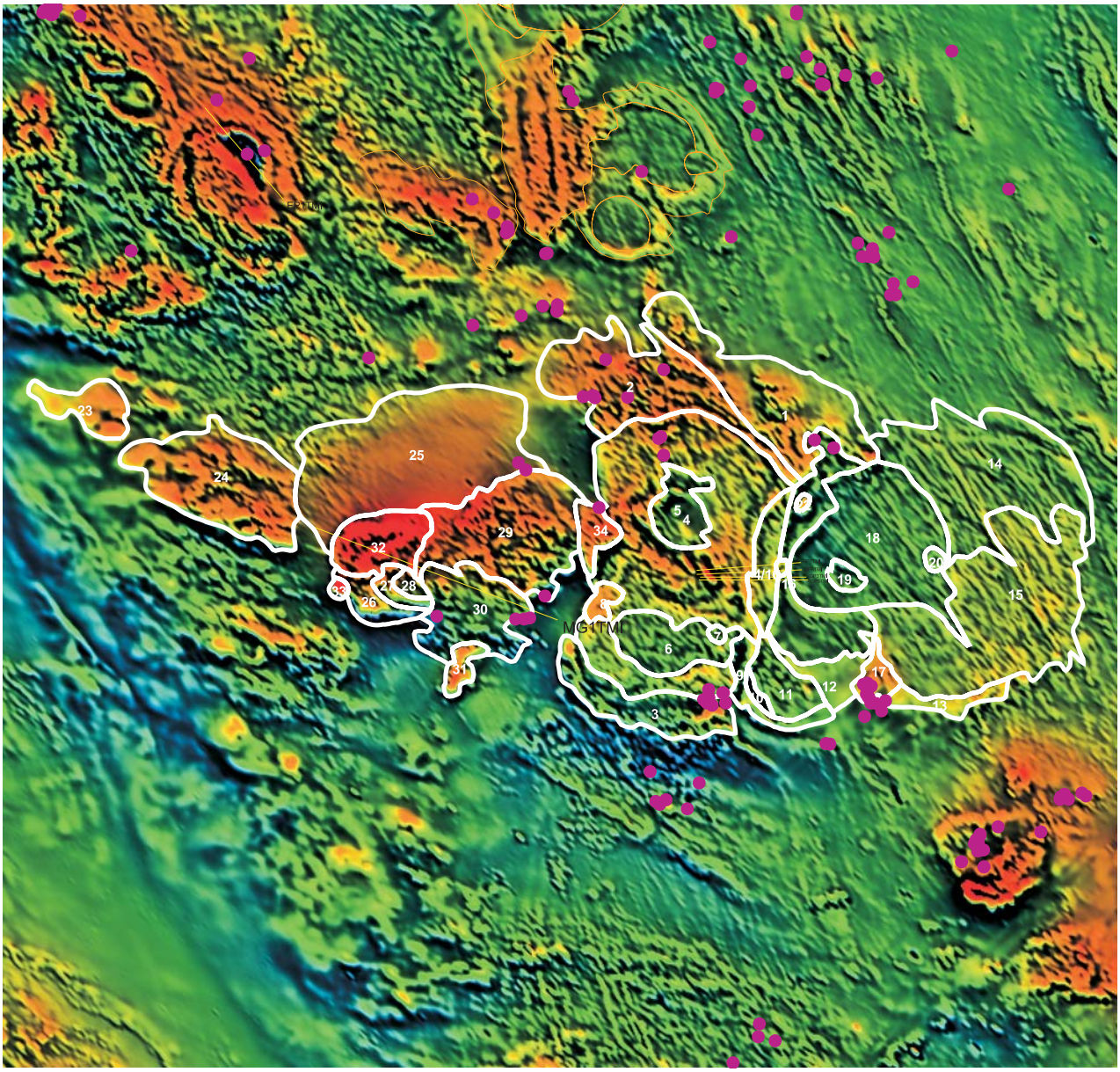


*Figure 11: Galloway Plains Igneous Complex (GP)*

*magnetism and includes part of body 2. The remainder of body 2 is interpreted as a contact aureole. Bodies 1, 3 and 4 are a diorite, which in body 1 includes large inclusions of layered gabbro like that of body 5. Body 6 is mapped as an unnamed intrusive diorite with a strong magnetic aureole. Body 7 does not crop out.)*

## Galloway Plains Igneous Complex (GP)

Coordinate at approximate centre: 276 000 E, 7 332 000 N

The Galloway Plains Igneous Complex comprises several phases that extend and join with the Craiglands Quartz Monzodiorite (refer geophysics GIS - theme gp_d.alg and Figure 11). Initial modelling was 2.5D (cross-section with limited strike) and focussed on several widely spaced east-west profiles across the centre of the intrusive body. Results were inconclusive, because of the complex relationships between phases in the centre of the body, which produced overlying magnetic responses, making the determination of the sequence of intrusive events difficult (refer geophysics GIS - model GP-A). AutoMag (refer geophysics GIS - model GP-B) highlighted several deeper bodies to the west with several near surface bodies in the main area of the intrusive complex. Interpretations of Forward modelling suggest that the shallower bodies have north-north-west strikes while the deeper rim anomalies strike north. 3D modelling using several close spaced lines (refer geophysics GIS - model GP-C) suggests two possible scenarios. The first has the eastern phase emplaced with subsequent normal faulting affecting its

western margin. The western phase subsequently intruded against this fault, overlying the deeper westerly dipping rim of the eastern phase. The alternative scenario has the western phase emplaced first with the eastern phase subsequently intruding. A high angle fault would then be required to lift the eastern side by at least 200m to produce the current configuration. This latter sequence of events is considered most likely because of faulting recognised in the area (274 800 E, 7 3237 000 N) and an associated change in depth of the rim of the eastern phase. The fault between the two phases was identified using radiometrics.

Timing relationships of the Galloway Plains Complex are as follows.

The earliest bodies are identified as 1 and 2. These may be the same phase but are separated by a fault. *(These bodies have been identified during mapping as contact metamorphosed rocks of the Rockhampton Group, Mount Alma Formation, Balaclava Formation and Raspberry Creek Formation.)* Their relationship to body 3 could not be established, but phases 1, 2 and 3 are all intruded by 4. *(The majority of body 4 equates to the Rocky Point Granodiorite, and body 3 is a contact aureole on the southern side of Galloway Plains Igneous Complex.)* It is possible that the dumbbell shape of 4 is the result of two separate intrusions but no boundary is evident and the composition of the northern and southern parts appears similar. *(Based on geochemical analyses parts of bodies 4, 6, 9 and 11 are differentiated as the Rocky Point Granodiorite.)* Body 5 intrudes 4 generating some magnetic alteration (Body 5 equates to the Redshirt Granite). Body 6 intrudes 4 and is intruded by 7. Body 8 also intrudes 4 and has a higher susceptibility. *(Parts of bodies 6 and 8 are mapped as Dumgree Tonalite.)* Whilst it appears that body 9 intrudes 6 and is intruded by part of 4 it is considered that 9 is in fact later than both 6 and 4, but that the margin of 4 overlies and obscures the margin of 9. Body 10 may be an alteration aureole around 11 or an earlier intrusion, which is almost entirely replaced by 11. *(Body 10 is mapped as a contact aureole in Youlambie Conglomerate.)* Body 11 intrudes 4, 9 and 10 and is intruded by 12 and 16. The boundary between 11 and 12 is largely faulted, but a portion of the contact that has not been faulted or affected by the contact aureole of 16 suggests that 12 intruded 11. Body 13 may be a contact aureole for 15 but because of its broader and less regular appearance than other aureoles it has been interpreted as a separate phase that is almost replaced by 15. Body 15 has a slightly more intense response than 14 and is interpreted to be a separate body.

Boundaries between 14 and 15 are faulted, however, in one location on 15's northern boundary (291 500 E, 7 335 600 N), the convex shape suggests that 15 has intruded 14. Body 16 intrudes 11, 12, 15 and 4. Body 17 may represent alteration that affects 12, 13, 15 and possibly 16. *(Bodies 14–16 and 18 and part of 12 are mapped as the Bocoolima Granodiorite, but poor outcrop has prevented geological subdivision of this intrusion. Bodies 13 and 17 represent a contact aureole about the Bocoolima Grandodiorite.)* Body 18 also intersects 16 and has an alteration rim. Bodies 19 and 20 both intrude 18. *(Body 19 equates to the Voewood Granite.)* Bodies 21 and 22 both intrude 16 and may be late events. *(Body 22 has been drilled and found to be granodiorite or tonalite no different from the Bocoolima Granodiorite. The magnetic body must lie at depth.)*

## Craiglands Quartz Monzodiorite (CIC)

Coordinate at approximate centre: 248 000 E, 7 334 000 N

The Craiglands Quartz Monzodiorite consists of a series of intrusions aligned roughly east-west. A model section was generated across bodies 32 and 30 (refer geophysics GIS — model CIC-A) that showed anomalies from magnetic units as close to outcropping in the west and progressively deepening to ~300m in the east. AutoMag modelling confirmed this trend and correlated well with results from the Forward modelling (refer geophysics GIS — model CIC-B).

The majority of the Craiglands Quartz Monzodiorite is interpreted to be older than the Galloway Plains Igneous Complex since body 34 of Craiglands is intruded by body 4 of the Galloway Plains Igneous Complex. *(Body 34 is in contact with the Dumgree Tonalite in outcrop and is included in the Galloway Plains Igneous Complex in geological reports. Body 34 is an unnamed gabbro.)* The oldest phase of the Craiglands Quartz Monzodiorite is interpreted to be in the west, body 23. This body is the deepest and likely to be the oldest intrusive phase if the general trend of intrusives becoming progressively younger eastwards, established in the Galloway Plains Igneous Complex, is followed. Body 24 is older than bodies 4 to 22. Relationships between 24 and bodies 1, 2, 3, 23 26, 27 and 28 could not be determined. Body 25 is deep, displays a

uniform response and appears to intersect 24. *(Bodies 23–25 are interpretations based purely on geophysics, with no surface indications of intrusions.)* No relationship could be established between 26 and 25, but body 26 is intruded by 27, which is in turn intruded by 28. Bodies 26, 27 and 28 are considered as separate bodies because of the variation in their susceptibilities (high in 26, low in 27 and moderate in 28) and because all bodies have alteration aureoles. A prominent low to the south of body 26 is interpreted to be the combined effect of 25, 26 and 32. *(Bodies 26, 27, 28 and 32 form the western part of the Craiglands Quartz Monzodiorite which is quite uniform in outcrop and magnetic susceptibility.)* Bodies 28 and 25 are intruded by 29, which is in turn intruded by 30. Bodies 29 and 30 are interpreted to be separate phases because of the sharp change in susceptibility across a clear boundary. *(Body 29 comprises the Smoky beds, the Inverness Volcanics, and the eastern part of the Craiglands Quartz Monzodiorite, most of which has much lower magnetic susceptibility than the western part.*) Body 30 is intruded by 31. *(Body 30 equates to the Smoky beds, and body 31 is an unnamed granodiorite.)* Body 32 intrudes all bodies from 25 through to 29. Bodies 31, 32 and 33 are considered to have significant magnetic alteration enhancement of their susceptibilities. *(Body 33 is a small gabbro intrusion that cuts the Craiglands Quartz Monzodiorite.)*

Body 34 intrudes 29 and is intruded by body 4 of the Galloway Plains Igneous Complex.

## Glassford Igneous Complex (GF)

Coordinate at approximate centre: 323 000 E, 7 290 000 N

The Glassford Igneous Complex comprises a series of intrusions for which the timing relationships have been inferred as follows (refer geophysics GIS — themes gf_c.alg, gftime.shp and Figure 12).

The oldest body in the complex is unclear and may be either 1, 2 or 3. No relationship could be established between these three. Body 1 is separated into parts a and b, which are interpreted as different phases brought in contact by a fault boundary. *(Bodies 1 and 2 crop out and equate broadly with Littlemore Granodiorite and the Lawyer Granite. The Littlemore Granodiorite comprises bodies 1, 13 and part of 4.)* Body 4 is younger than 2. *(Body 4 also includes the Rule Gabbro, part of the Lawyer Granite and country rock of the Rockhampton Group.)* No relationship could be established between bodies 1, 3 and 4. Body 5 is interpreted as being younger than 4 based on the relationship and nature of the contact at the western margin. Body 6 intrudes 4 but does not appear to intersect 5. It is not clear whether 7 intrudes 6, but both are intruded by 8. *(Bodies 5, 6 and 7 largely comprise country rock, some of which may be aureoles. Body 8 is the Monal Granodiorite which is surrounded by a strongly magnetic contact aureole in the Three Moon Conglomerate.)* Body 3 is intruded by both 7 and 15. *(Body 15 is a Tertiary basalt plug at Pine Mountain.)* Body 9 was interpreted to be later than both bodies 4 and 6. *(Body 9 includes the Burns Spur Nephaline Monzosyenite and parts of the Ridler Monzonite and the Monal Granodiorite.)* Body 11 intrudes bodies 4, 6 and 9. Body 12 is very magnetic and may be a gabbro, skarn or alteration effect that cuts across body 5. *(Body 12 comprises the Radley Nephaline Syenite and part of the Ridler Monzonite. Body 11 largely comprises Ridler Monzonite.)* Body 13 intrudes 4, 5 and 1a and is in turn intruded by 14. Body 14 has a very intense alteration aureole with amplitude similar to body 12. *(Body 14 is mapped as the Robert Granite and is surrounded by a pronounced magnetic high related to a gabbro, which is exposed mainly to the south of the granite.)* Intrusions 16 and 17 being physically separated from the other bodies had no timing relationship established. Body 17 is subdivided into two parts, a and b, because of slightly different magnetic responses and a faulted contact between the two. *(Body 16 equates to the Munholme Quartz Diorite, which is surrounded by a relatively wide magnetic contact aureole.)*

Forward modelling of the complex across the strongly magnetic rim around the Robert Granite used vertical dips to provide indications of depth, which varied from 250m on the north-west rim to 500m on the south-eastern rim. Depths of around 700m were modelled in the north-east of the complex. *(The Rule Gabbro outcrops in the south-east, suggesting that the exposed rocks are not the sole source of the anomaly and that more magnetic rocks occur at depth.)* While most of the models had susceptibilities consistent with those measured in the field, some were higher by a factor of 2, suggesting that modelling depths may be too large. AutoMag solutions matched the Forward model fairly well when constrained by vertical dips. When the correlation between the model and data allowed dips to be free, AutoMag solutions were slightly deeper than the Forward

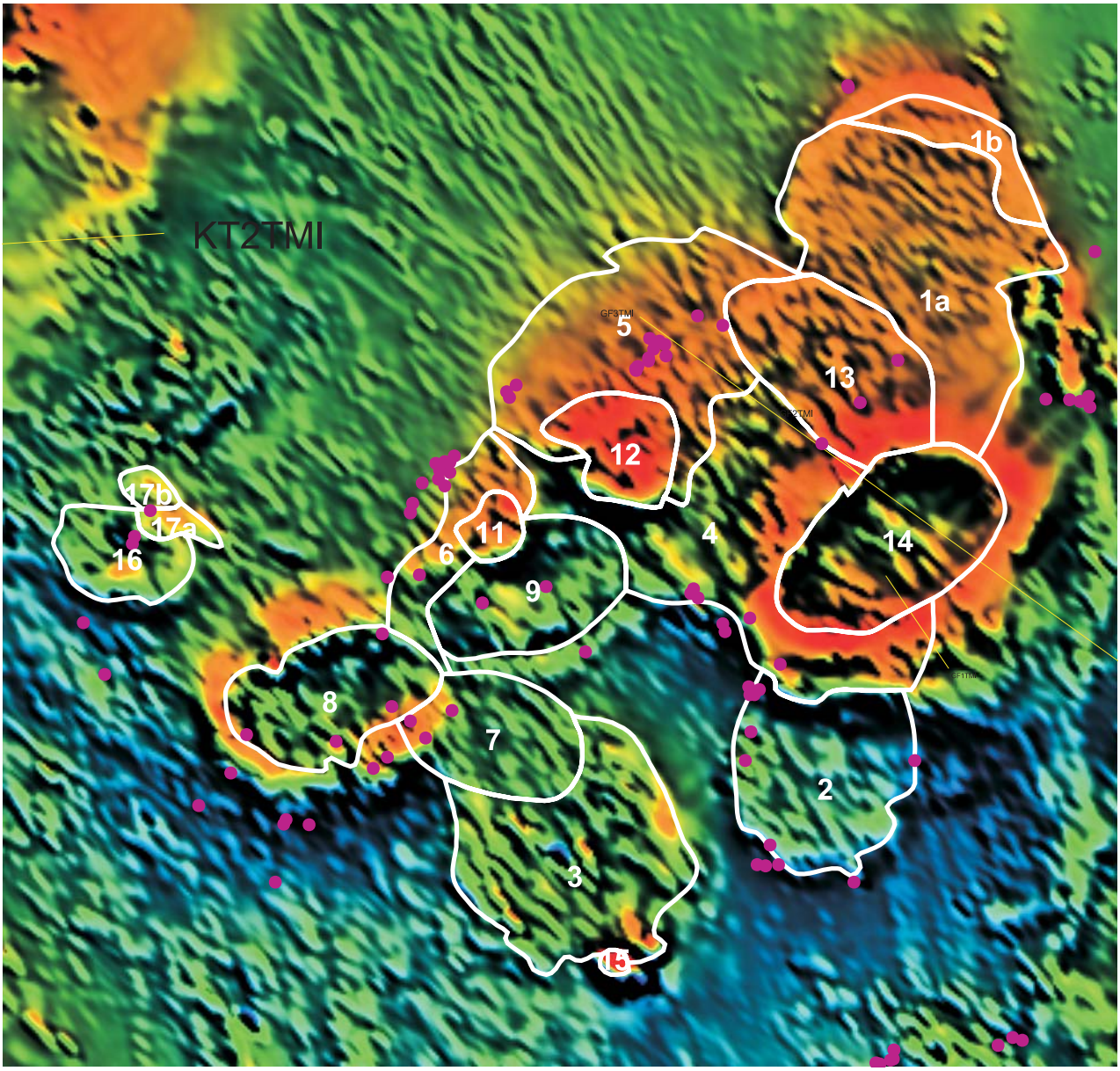


*Figure 12: Glassford Igneous Complex (GF)*

modelling and dipped steeply to the south-east.

## Bajool (BJ)

Coordinate at approximate centre: 255 000 E, 7 378 000 N

The Bajool Quartz Diorite and Cecilwood Quartz Diorite are discussed together because they form a continuous magnetic feature. The gravity interpretation, however, indicates a major fault and gravity ridge between the two. The gravity data also suggests that the Cecilwood Quartz Diorite is physically linked to and similar to the Galloway Plains Igneous Complex.

The timing relationships for the various interpreted phases (refer geophysics GIS — themes bjtime.shp, bj_c.alg) are as follows.

Body 1 is interpreted to be the oldest, with all others bodies either intersecting it directly (2, 3, 4 and 5) or intruding bodies that do. Body 2 intersects 1 and is in turn intersected by both 3 and 5.

*(Bodies 2 and 4 are mapped as a continuous intrusive phase, the Cecilwood Quartz Diorite, with body 1 primarily comprising surrounding contact aureole.)*

It is not clear whether body 5 is a separate intrusion or simply represents the effect of alteration enhancement of susceptibilities. *(Body 5 is comprised largely of Devonian gabbro*

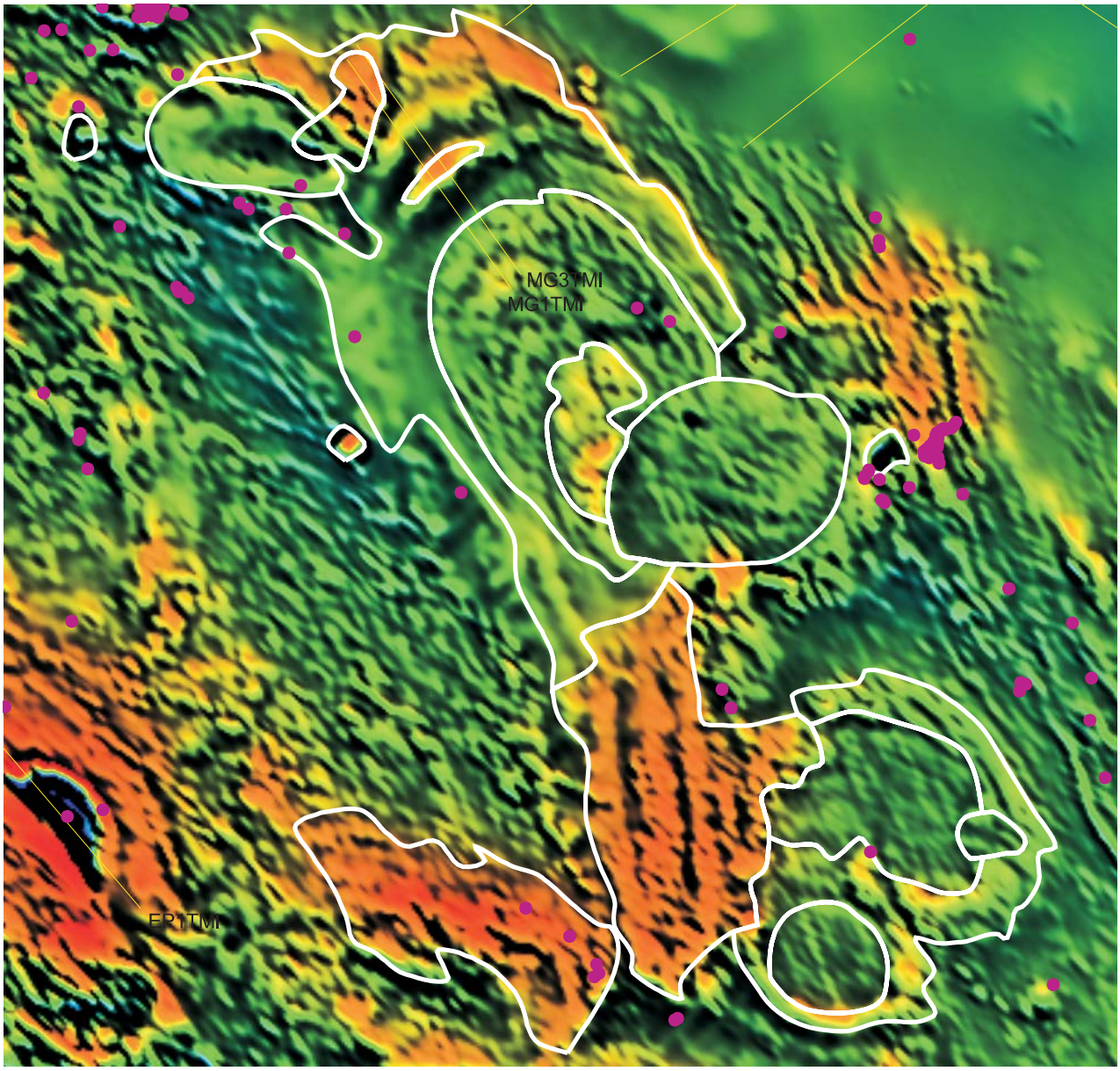


*Figure 13: Bajool Quartz diorite — Cecilwood Quartz Diorite (BJ)*

*and in the north, some Bajool Quartz Diorite.*) An internal fabric with a north–south strike is evident. This body may represent the effects of a deeper intrusive body. Body 5 is intersected by 6 *(mapped largely as alluvium with Capella Creek Group in the west and Bajool quartz Diorite in the east)*. Body 7 may be a separate phase or a shallow part of 6. Body 8 intrudes 7 and body 9 intrudes both 7 and 8 (Bodies 7 and 8 are mapped as alluvium with some of the Bajool Quartz Diorite cropping out in 9.) Body 10 is interpreted as a possible skarn or alteration zone. Body 11 intrudes 6 and is intruded by 12. Body 12 may be a separate intrusion or represent an alteration zone. *(Body 12 is mapped as alluvium and Mount Alma Formation.)* Body 13 is a separate small intrusion, which has a weak aureole *(mapped as Raspberry Creek Formation)*. Body 14, as with 5 and 12, may be an intrusive phase or reflect alteration enhancement of susceptibilities. *(Body 14 includes Capella Creek Group and a small area of unnamed Permo-Triassic granite.*) Bodies 15 and 16 are interpreted as small intrusions. Body 15 has a sharp high and is either an outcropping unit such as a dyke or an artifact from culture such as a power line. It shows as a weak linear anomaly striking north-north-west. Body 16 is thought to be a small gabbro with negative remanence. *(Body 16 is mapped as Bajool Quartz Diorite and 15 as a rhyolitic volcaniclastic of the Mount Warner Formation.)*

AutoMag modelling in the north (refer geophysics GIS — model BJ-A) indicates steep northly dips with the exception of a strong anomaly in the centre of the line, which dips steeply to the south. A gentle deepening of the

body to the north is indicated. Forward modelling confirms the AutoMag solutions (refer geophysics GIS — model BJ-B) with depths varying from ~350m at the southern end of the line to >500m towards the northern end. At the very northern end the anomalies shallowed as the line crossed to another phase. The central anomaly when compared with all other anomalies in the area is interpreted to be shallower and dipping south rather than north. This feature is considered to represent either alteration or skarn development. Depth was modelled at ~400m but it is likely that it is in reality shallower than this, given that alteration and skarn magnetite are both likely to have diffuse boundaries.

## *Basins*

### Casuarina Basin (CB)

Coordinate at approximate centre: 267 000 E, 7 391 000 N

The largest basin in the area, the Casuarina, appears to have significant faulting both at the margins and within the basin, with the basement stepping to a maximum depth of almost 2000m. Forward modelling suggests basement depths of 1600m. Naudy modelling suggests a slightly shallower basement depth of 1520m while Fourier analysis had high confidence results at 1580m and 2000m.

At the very edges of the basin, the western side appears to have a sharp faulted contact with basement rocks while the eastern margin appears to dip gently under cover for several kilometres. This is consistent with previous interpretations of the basin as a Tertiary half graben with a fault on the western margin and gentle dips on the eastern margin.

### Jim Crow Basin (JC)

Coordinate at approximate centre: 258 000 E, 7 430 000 N

Modelling using Fourier analysis of the Jim Crow Basin shows magnetic layers at ~1700m and 350m.

### Nagoorin Basin (NB)

Coordinate at approximate centre: 330 000 E, 7 303 000 N

The Nagoorin Basin has numerous intrusions and near surface features making it difficult to accurately estimate basement depths. An area near the northern margin, relatively clear of near surface noise, was used for Fourier analysis. Results indicate a depth of between 600m and 650m but show all layers as low confidence.

### Parkhurst 'Basin' (PB)

Coordinate at approximate centre: 241 000 E, 7 423 000 N

Fourier analysis over the Rockhampton Group gives a moderate confidence layer for basement at 1186m. The moderate confidence layer correlates well with Forward modelling, which shows basement down faulted by ~300m on the western side and stepping down further to 1000m before rising gradually to the east. AutoMag solutions suggest depths that are ~200–300m shallower.

*(The Parkhurst 'Basin' is actually a belt of non-magnetic Rockhampton Group flanked to west and east by younger, more strongly magnetic units. The nature of the basement to the Rockhampton Group is unknown. This geophysical interpretation is not considered viable.)*

### Rossmoya Basin (RB)

Coordinate at approximate centre: 237 000 E, 7 448 000 N

Forward modelling of the Rossmoya Basin suggests sediment thicknesses of 300–400m. The basin appears uniform in a north–south direction but deepens slightly going in a west–east direction. AutoMag solutions correlates well with Forward modelling results in the western half of the basin, but suggests depths 250m deeper in the eastern half. Fourier analysis indicates moderate confidence layers at 91m and 2183m.

### Stanwell Basin (SB)

Coordinate at approximate centre: 225 000 E, 7 398 000 N

Forward modelling of the Stanwell Basin suggests basement depths of not more than 300m. Basement dips are consistent with an anticline in the centre of the basin and vertical dips on each end of the line.

### Yaamba Basin (YB)

Coordinate at approximate centre: 228 000 E, 7 440 000 N

Forward modelling of the Yaamba Basin suggests depths of up to 1300m. AutoMag generated depths of ~1300m but with sources at between 400 and 700m. These shallow sources may be basement, the effect of noise or possibly weak magnetic layers such as thin basaltic layers within the sediments. Fourier analysis suggests layers at 145m and 765m, which correlate to the shallower sources in the AutoMag modelling. Considering results from all modelling, sediments are considered likely to a depth of 1300m.

## GRAVITY INTERPRETATIONS

The gravity dataset was analysed using linears and closed anomalies. The colour scale for both the interpretation and the image has hotter colours representing higher values and cooler colours representing lower values (refer GIS theme Gravity.alg). The closed anomalies were defined using three gradational levels: from weak to moderate to strong. These interpretations are subjective and are only meant to convey local information. Relativities between anomalies can be gained from the gravity interpretation image rather than the line interpretations. Gradient and undifferentiated linears (often represented by a series of gradient features interspersed with either high or low features) are interpreted to be faults. In some instances, gradients may be in the opposite sense on different parts of a linear, this is attributed either to cross-cut faulting causing different blocks to have different a sense of throw or the fault being the boundary for intrusions.

### *Faulting*

Two linear highs extending north-north-west from the Nagoorin Basin are interpreted as thrust fronts. The strong low east of the Glassford Igneous Complex extends eastwards under the interpreted thrust front.

### *Intrusives*

A large negative anomaly evident in the data is identified as the Rawbelle Batholith. The north-eastern boundary of this body is interpreted to be fault controlled.

The Kroombit Tops area overall gives a weak low response but has a moderate gravity low associated with its eastern edge. This can be interpreted as the root of an intrusion on the eastern side or evidence of a separate intrusive phase.

The Diglum area does not show up as a significant anomaly.

The Glassford Igneous Complex appears relatively neutral in the gravity data apart from phase 3, which is a weak low and phase 12, which appears as a weak high. The complex overlaps a strong low to the east, which also covers the Nagoorin Basin. However, neither the complex nor the basin is thought to be the origin of the low, which is offset and larger than both features. The low is interpreted to be another batholith at depth.

The Galloway Plains Igneous Complex has a moderate low centred beneath body 18. The remainder of the complex appears as a weak gravity response.

The Cecilwood Quartz Diorite appears connected to the Galloway Plains Igneous Complex in both the magnetic and the gravity data, the latter not only suggesting a physical connection with a weak low extending about and enclosing both complexes but also a similar composition for both complexes.

A weak gravity high encloses both the Craiglands Quartz Diorite and the Eulogie Park Gabbro. The Eulogie Park Gabbro is a very intense magnetic anomaly with strong remanence consistent with a basic intrusion.

The southern part of the Bajool Quartz Diorite intrusive complex shows a weak gravity low. It does not extend north-west into the region of strong magnetic banding visible in the magnetic data, suggesting that the bands are not rims within the intrusion but probably represent magnetic skarn or alteration development.

The Bouldercombe Igneous Complex gravity signature has the main east and west lobes appearing as lows relative to highs that surround them. A gravity high along the

northern edge of the outcropping area is interpreted to correspond to the magnetic body 1. A strongly magnetic body 19 has a strong gravity high immediately west of it suggesting that it may be a basic unit.

Moderate to strong gravity highs within and north of the Rookwood area are thought to be basic intrusives.

A relative low north of Ridgelands is coincident with an intrusion. The low does not extend to the south-west where different phases of the intrusive complex have been interpreted using radiometric data.

### *Basins*

The Casuarina, Yaamba and Nagoorin Basins appear as obvious gravity lows. A weak low is evident in part of the Jim Crow Basin, but the Rossmoya and Stanwell Basins show no obvious gravity response.

## RADIOMETRIC INTERPRETATIONS

A three channel red-green-blue mix was used for the interpretation (refer GIS theme Radiometrics.alg). The radiometric channels were converted to ppm for uranium and thorium and to percent for potassium. In areas where greater contrast was required the image window was zoomed in to the specific area and an automatic 90% clip was applied to all channels and new ratios were generated.

A surface map of the area was generated using the above datasets (refer GIS theme Radiometrics.shp). Boundaries of radiometric zones were interpreted with solid lines. These included areas of water such as dams, rivers and the coast. Some features, in particular thin linear highs or lows in one or more radiometric channels, are interpreted as structural zones and are marked with dashed lines.

These zones are considered as representing areas where ground water has either enhanced or depleted radiometric elements in the near surface.

## AREAS PROSPECTIVE FOR MINERALISATION

A number of areas were identified as prospective based on the geophysical interpretation of alternation, skarns and/or structural zones (refer geophysics GIS — prospects theme).

Structural zones were identified in the Kabra Quartz Monzodiorite in bodies 1b, 2, 8b and 15. Zones of possible alteration were also identified in the Moonmera Porphyritic Granodiorite and the Bundaleer Tonalite (refer Figure 14).

Areas prospective for skarn were identified in the north of the Diglum Granodiorite in bodies 2 and 6 (Figure 15).

An area of potential skarn development was identified in body 1 of the Gallowplains Igneous Complex, at the contact between an unnamed Permian limestone unit and an unnamed Permo-Triassic granitoid. Structural zones with potential for mineralisation were identified bounding bodies 1 and 34 and at the contact of the Inverness Volcanics (body 29) and the Dumgree Tonalite (body 30) (Figure 16).

An area of possible skarn development is identified in body 15 of the Glassford Igneous Complex, a basalt plug in contact with Rockhampton Group.

Possible skarn development is identified under recent cover in or adjacent bodies 6 and 9 of the Bajool Quartz Diorite (Figure 18).

West of the Ridgelands Granodiorite and at the western contact of the granodiorite areas of alteration and skarn have also been identified.

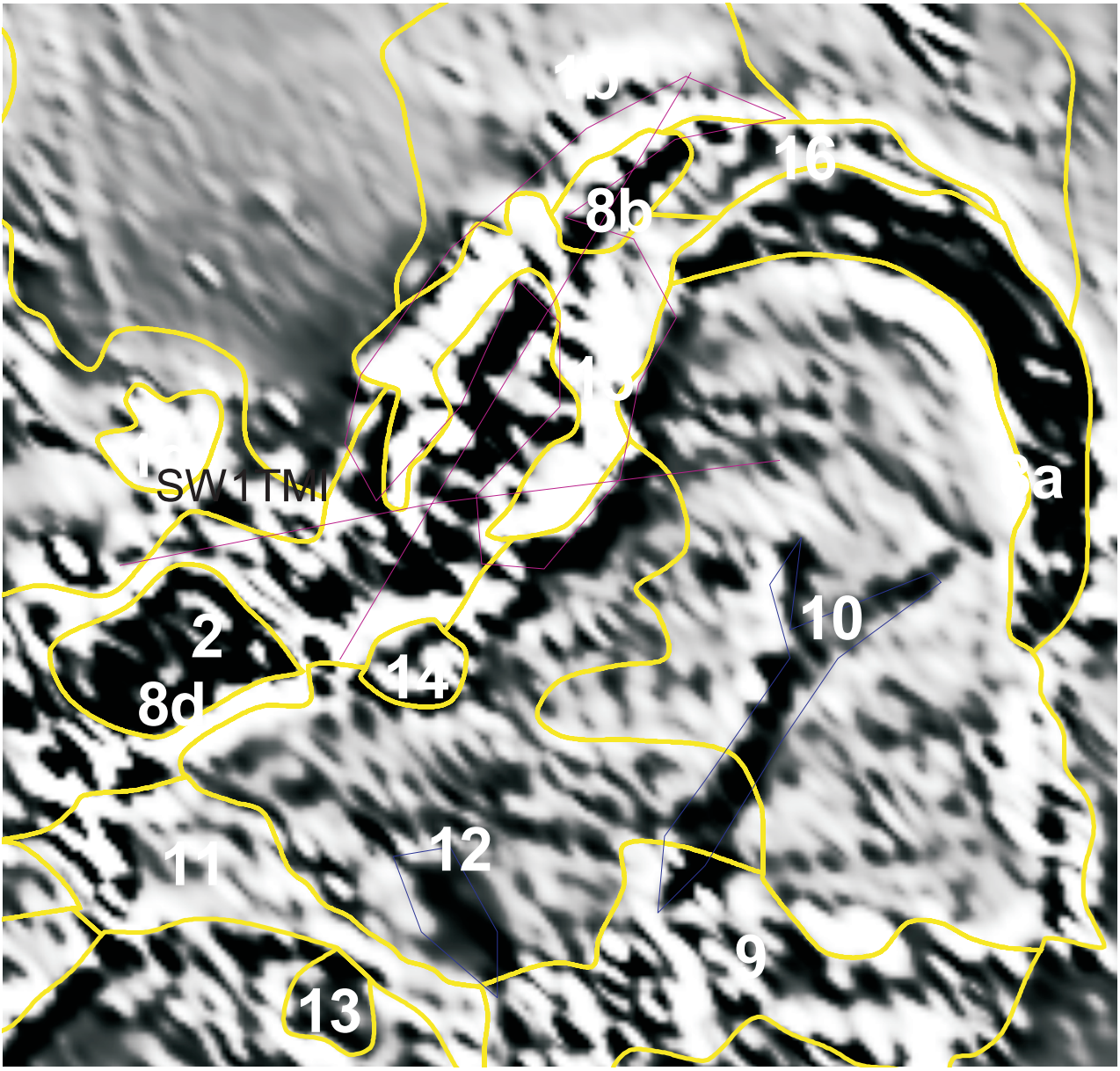


*Figure 14: Bouldercomb Igneous Complex prospective areas*

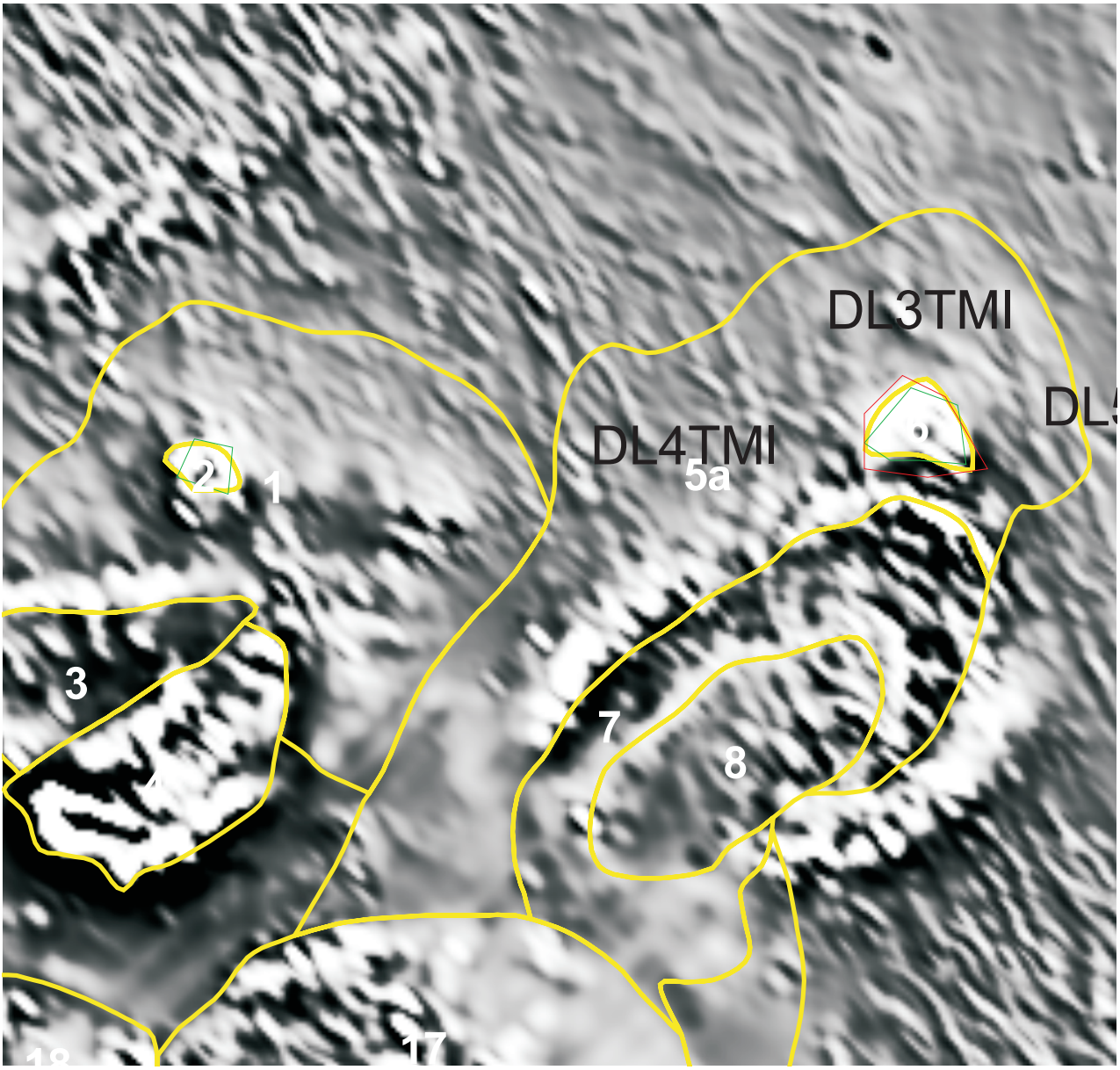


*Figure 15: Diglum Granodiorite prospective areas*

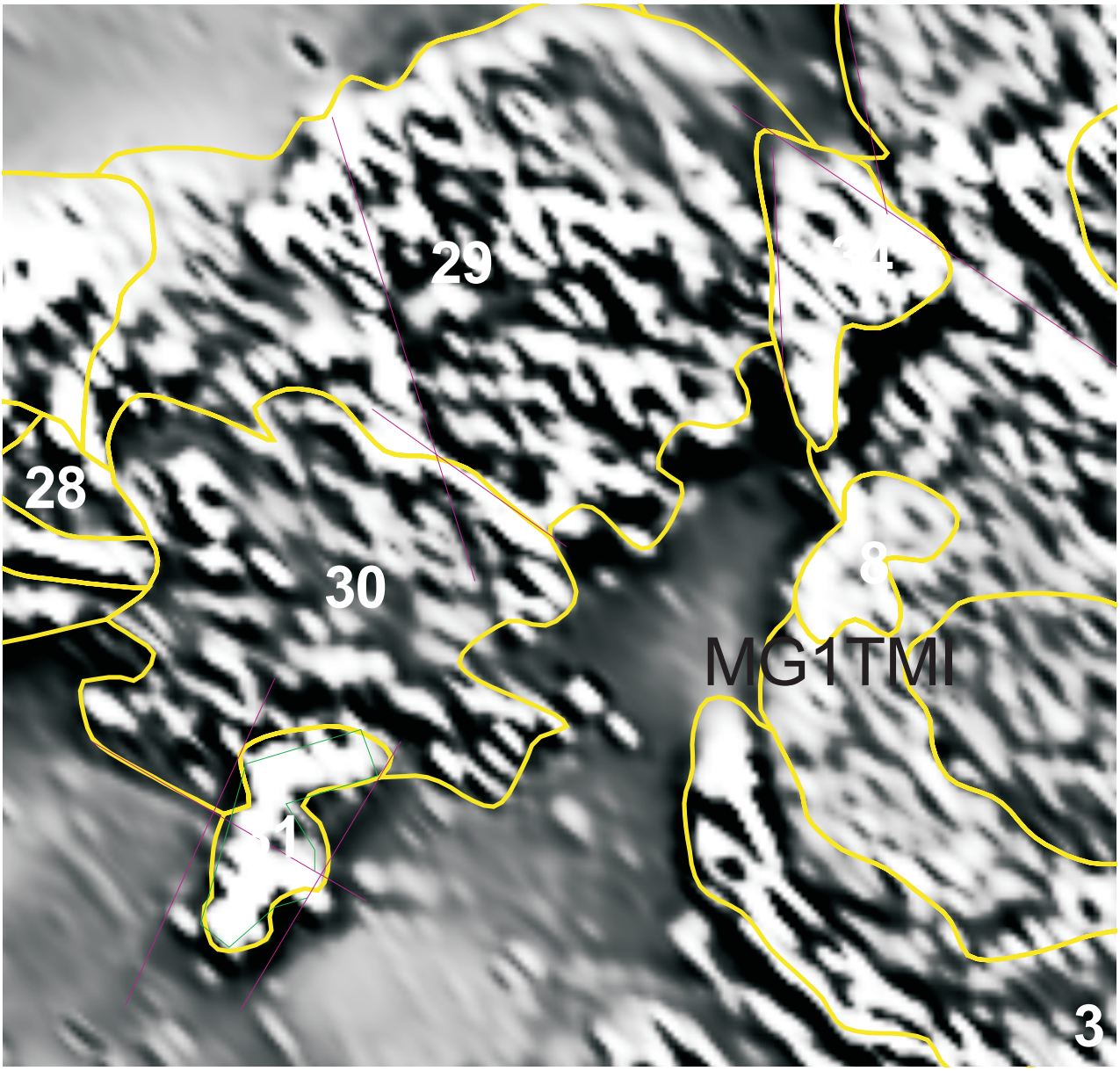


*Figure 16: Galloway Plains Igneous Complex prospective areas*

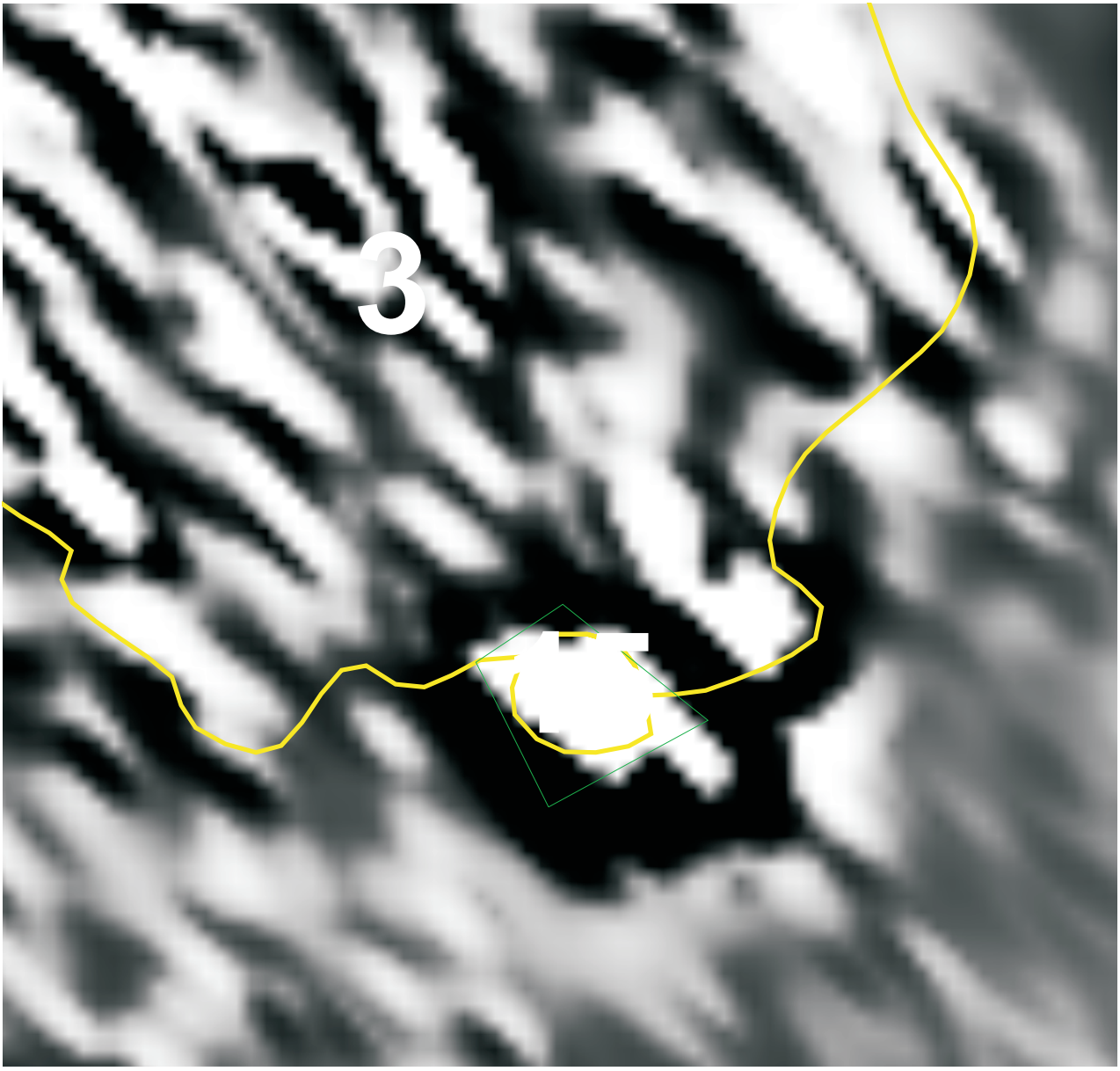


*Figure 17: Glassford Igneous Complex prospective areas*

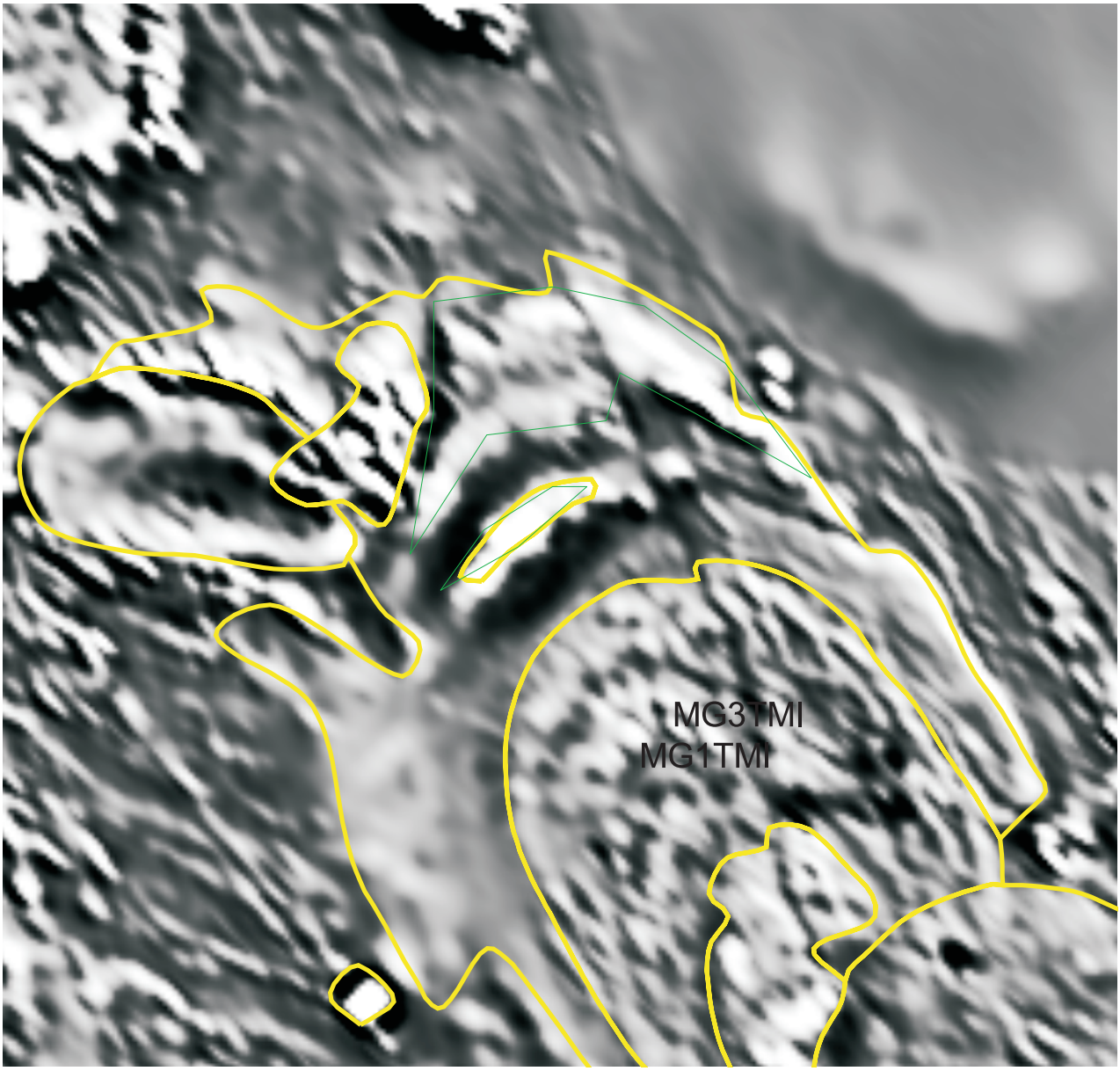


*Figure 18: Bajool Quartz Diorite prospective areas*